

Development and validation a novel copper death and SARS-CoV-2-associated genes prognostic model in hepatocellular carcinoma

congzhi yan

First Affiliated Hospital of Wenzhou Medical University

zhixuan wu

First Affiliated Hospital of Wenzhou Medical University

donghao lou

First Affiliated Hospital of Wenzhou Medical University

Jingji Jin

First Affiliated Hospital of Wenzhou Medical University

Congcong Wu (✉ wucongcong@wzhospital.cn)

First Affiliated Hospital of Wenzhou Medical University

Research Article

Keywords: Copper death, liver cancer, prognostic, SARS-CoV-2

Posted Date: April 7th, 2022

DOI: <https://doi.org/10.21203/rs.3.rs-1519044/v1>

License: © ⓘ This work is licensed under a Creative Commons Attribution 4.0 International License. [Read Full License](#)

Abstract

Copper death is a newly identified unique form of regulated apoptosis. Studies suggest that it may be the mode of apoptosis in cancer cells. Therefore, copper death-related genes may become therapeutic targets for hepatocellular carcinoma. Also, SARS-CoV-2 is currently the most widely spread virus in the world with no curative drug available. Liver cancer is the most common fatal malignancy in the world. By the time a patient presents to the clinic, liver cancer has progressed to an advanced stage and the prognosis is often poor. In this study, the prognosis of patients with liver cancer when they get SARS-CoV-2 was predicted by examining the relationship between SARS-CoV-2, copper death and liver cancer.

1. Introduction

Hepatocellular carcinoma is one of the most common cancers in the world and its incidence is increasing year by year[1]. Hepatitis B virus, hepatitis C virus, alcohol, and other factors cause liver cancer, while in China, there are about 200 million hepatitis B patients. These patients will eventually develop liver cancer. Diagnosis of hepatocellular carcinoma the most commonly used biological marker for liver cancer is now alpha-Fetoprotein (AFP)[2], but the diagnostic efficacy of AFP is limited[3-6]. And treatment of hepatocellular carcinoma mainly includes liver transplantation, hepatectomy, radiofrequency ablation, hepatic artery chemoembolization (TACE), and radioembolization, and the choice of these treatments modalities depends on the load and location of the hepatocellular carcinoma[7]. Current treatment has seen rapid growth in HCC immunotherapy research in the last decade and has changed the treatment paradigm, with immune checkpoint inhibitors (ICIs) having been identified for the treatment of advanced liver cancer [8-12]. However hepatocellular carcinoma still is the second most common cause of cancer death worldwide[13]. Therefore, it is necessary to determine the survival time of each patient to reduce the burden on each family.

Copper ions are an essential component for the survival of every cell in the body[14]. Normal cells are able to maintain intracellular copper ion levels at a healthy level [14-17]. When the intracellular concentration of copper ions rises to a certain level, copper ion carriers will regulate cell death in a distinct form targeting lipoylated TCA cycle proteins [18].

SARS-CoV-2 is still prevalent worldwide and is causing significant economic stress and burden on people [19, 20]. Although there is now a vaccine against SARS-CoV-2 that boosts immunity to the virus [21-25], many countries are still in the midst of a serious epidemic and there is no cure for SARS-CoV-2 in the short term.

In this study, we obtained RNA-seq data and clinical data from public databases to investigate a copper death and SARS-CoV-2 related prognostic model to predict overall survival in patients with hepatocellular carcinoma. High-risk scores were associated with advanced clinicopathological features and poor prognosis. The reliability of the model was developed and validated.

2. Methods

2.1 Publicly available data and processing

The gene expression and clinical information were obtained from The Cancer Genome Atlas project (<https://cancergenome.nih.gov/>), including 374 Liver cancer samples and 50 normal samples. Gene expression profile data for GSE4236(n=81) were downloaded from the Gene Expression Omnibus (GEO) database (<https://www.ncbi.nlm.nih.gov/geo/>). We used annotation files to convert the identification probes into gene symbols. To identify the DRGs, we applied the R software "limma" package with a criterion of |fold change| greater than or equal to 1.5 and an adjusted p-value of <0.05. Differentially expressed copper death genes between LIHC tissue and normal liver tissue were analyzed. Patients with TCGA were classified according to differentially expressed genes associated with copper death. The differential genes in the different subgroups of patients were then analyzed and these genes were used as alternative genes for our model. The TCGA dataset was used as a training group and the GSE54236 dataset from the GEO database was used as a validation group. Institutional ethics committee approval was not required for the current study for the TCGA and GEO are publicly available.

2.2 SARS-CoV-2 related gene screening and Risk score establishment

Selected overlap of SARS-CoV-2 related genes and differentially expressed genes. A follow-up analysis was done based on these overlapping genes. In addition, SARS-CoV-2 related genes were selected from the OMIM database, the Genecard database, and NCBI gene junction module. All genes associated with prognosis were screened by univariate Cox regression analysis. After this, we used a lasso Cox regression analysis to pick out the best genes. The LASSO regression model was used to calculate the coefficients for each gene. The equation for the prognostic model: risk score = gene^A expression × corresponding coefficient + gene^B expression × corresponding coefficient + gene^C expression × corresponding coefficient + ... + gene^Z expression × corresponding coefficient. Patients were divided into high-risk and low-risk clusters based on the median risk score. Kaplan-Meier survival curves and time-dependent ROC curves were used to compare survival differences between the two clusters and to assess the predictive power of the model using the 'survival ROC' package respectively.

2.3 External validation of prognostic

GSE54236 was used for validation. The same copper death and SARS-CoV-2 related prognostic genes were used to calculate a risk score for each patient. Risk scores were used in ROC curves and Kaplan-Meier analyses.

2.4 Stratification analysis of the copper death and SARS-CoV-2 related prognostic signature

To explore the impact of prognostic genes on the clinicopathological characteristics of gastric cancer, we assessed risk scores against six clinicopathological factors (age, sex, grade, stage, T-stage, M-stage, and N-stage).

2.5 Gene Ontology (GO) and Kyoto Encyclopedia of Genes and Genomes (KEGG) Functional Enrichment Analysis

The "limma" package and the "clusterProfiler" R package were used to analyze the differences between high- groups and low-risk groups, GO and KEGG-related enrichment pathways. Control the FDR and adjust the P-value according to the BH method.

2.6 Immune infiltration analysis

To distinguish between immune cell infiltration in the TCGA and GEO databases, we calculated the infiltrating score of 16 immune cells, and 13 immune-related pathways separately. These correlation analyses were inferred from the gene expression of LIHC by single-sample gene set enrichment analysis (ssGSEA)[26].

2.7 Statistical Analysis

We applied Student's t-test to distinguish genes differentially expressed in tumor and normal tissues. differences in ssGSEA scores of immune cells or pathways between risk groups were assessed by the Man-n-Whitney test, with p-values adjusted by the BH method. Kaplan-Meier analysis and the log-rank test were used to compare OS between groups. independent predictors of OS were identified by univariate and multivariate Cox regression analysis. All statistical analyses were performed using R software (version 4.1.1). Differences were considered statistically significant when the p-value was less than 0.05.

3. Results

3.1 Identification of differentially expressed genes and classification of patients

To investigate the expression of genes associated with copper death in HCC, we compared relevant genes in normal and tumour tissues. The results revealed that LIAS, LIPT1, DLD, DLAT, PDHA1, PDHB, MTF1, GLS, and CDKN2A were highly expressed in tumour tissues and FDX1 in normal tissues (figure 2a, 2b). We also showed the correlation between the 10 genes (figure 2c). Based on the 10 genes, we divided the patients into three categories (figure 2d) and analysed the overall survival (OS) between them and found P<0.001 (figure 2e).

3.2 Development and validation of a prognostic model for copper death and SARS-CoV-2 association

The analysis identified 2443 differentially expressed genes between the three patient groups, which were found to be mainly associated with T-stage, stage, and gender (figure 3a). These genes were intersected with SARS-CoV-2-related genes, and there were 275 intersected genes in total (figure 3b). A single gene prognostic regression analysis was done based on the 275 genes and all 62 genes $P < 0.01$ were associated with prognosis (figure 3c). Using these 62 genes for lasso regression analysis and lasso regression models (figure 3d, 3e), four genes were finally identified as our prognostic model risk score = $SSX2IP * 0.00100336665126057 + RNF145 * 0.040899709061588 + GTSE1 * 0.120514296049806 + SLC1A5 * 0.166208688574242$. Patients with TCGA and GEO were scored according to these four genes. The difference in their OS was by significance, $P < 0.001$ for the training group (figure 3f), $P = 0.01$ for the validation group (figure 3g).

3.3 Analysing the effects of prognostic models

The training and validation sets were analysed for area under the curve (AUC) and the AUC for the training set was found to be 0.804 (figure 4a), a very high value, and 0.676 (figure 4b) for the validation set. PCA (figure 4c-d) and t-SNE (figure 4e-f) analyses of patients in the high-risk and low-risk groups demonstrated a significantly different distribution of patients in the two groups. The validity of our model was further confirmed. Finally, we did a single-factor regression analysis (figure 4g) and a multi-factor regression analysis (figure 4h) of the riskscore. Again, it was validated that our riskscore can be used as an independent predictor of patient prognosis as well as clinical characteristics.

3.4 Clinical correlation and associated pathway analysis of 4 genes

SSX2IP, RNF145, GTSE1, SLC1A5 major T staging, stage staging, grade grading, gender related (figure 5a) were found. After this, all differential genes were analysed for related pathways and found to be enriched in the Biological Process mainly in the fatty acid metabolic, mitotic nuclear division pathway, and in the Cellular Component mainly in the chromosome, The cellular component was mainly enriched in chromosome, centromeric region, collagen-containing extracellular matrix, oxidoreductase activity, acting on CH-OH group of donors was enriched in Molecular Function (figure 5b, 5c). In KEGG-related pathways, the main focus is on Metabolism of xenobiotics by cytochrome P450, Drug metabolism - cytochrome P450, etc. (figure 5d, 5e).

3.5 Analysis of immune infiltration of TCGA and GEO

Analysis of 16 immune cells and corresponding immune pathways in patients with TCGA showed that aDCs, iDCs, macrophages, neutrophils, NK cells, T helper cells, Tfh, Th2 cells, TIL and Treg cells were significantly elevated in the high-risk group (figure 6a). There were also corresponding differences in 11 of the 13 immune pathways (figure 6c). This suggests that immune factors may be an important factor in the prognosis of patients. Correspondingly, five immune cells were also upregulated in the high-risk group in patients with GEO (figure 6b), and eight immune-related pathways were also differentially represented (figure 6d).

3.6 Predicting drug sensitivity and drug correlation analysis

By predicting 12 drugs, we found that six were more effective for the low-risk group (figure 7a-f) and, similarly, six were more effective for the high-risk group (figure 7g-l). Drug correlations were analysed for four genes and figure 8 showed that 16 drugs were associated with different genes.

4. Discussion

In this study, we first analysed their expression in hepatocellular carcinoma species through the 10 copper death-related genes obtained. It turned out that all genes were differentially expressed in the tumours. Afterwards, these 10 genes were used to classify patients into 3 categories, and there was a difference in survival between these 3 categories of patients. Currently, the world is in the midst of a covid-19 epidemic. To further investigate copper death and covid-19-related genes in the prognosis

of patients with hepatocellular carcinoma, we have developed a prognostic model consisting of four labels, which has been validated by an external dataset.

There are four genes (SSX2IP, GTSE1, SLC1A5, RNF145) in our copper death and Covid-19 related prognostic model. Three of four (SSX2IP, GTSE1, SLC1A5) have been shown to be associated with the development or metastasis of liver cancer [27-33]. And RNF145 regulates cholesterol in cells through the sterol-responsive Liver X Receptors (LXRs) [34]. LXRs play a critical role in regulating cellular cholesterol. It was found that inactivation or knockdown of RNF145 expression enhanced cholesterol biosynthesis gene expression and increased liver and plasma cholesterol levels [35]. RNF145 controls cholesterol levels through intact SREBP signaling (SREBP2). Studies suggest that RNF145 is associated with cholesterol regulation [36, 37]. A study in Xinjiang, China, showed that mutations in RNF145 affect changes in blood lipids [38]. Diets high in cholesterol promote the progression of liver cancer through the Penny Flora [39]. Similarly, dietary cholesterol promotes steatohepatitis-associated hepatocellular carcinoma through metabolic dysregulation and calcium signaling [40]. Therefore, RNF145 can indirectly influence the development of hepatocellular carcinoma by affecting cholesterol and thus hepatocellular carcinoma. In our study, the coefficient of RNF145 was only 0.04, which is much different compared to GTSE1, SLC1A5. On the other hand, RNF145 is mainly associated with cholesterol transport and influences the concentration of cholesterol in the blood. So this prognostic model associated with copper death and SARS-CoV-2, is still reliable.

Synovial sarcoma, X breakpoint 2 interacting protein (SSX2IP) is also expressed in many cancers and its high expression shows poor patient prognosis [27, 41-43]. SSX2IP has been shown to be a potential target for immunotherapy in leukaemia [42]. High expression of SSX2IP in hepatocellular carcinoma would imply larger tumors, more cancer thrombi, and shorter survival times. Also, elevated expression of this gene promotes hepatocellular carcinoma metastasis in the peritoneum and liver metastasis. High expression of SSX2IP stimulates wound healing, metastasis, and invasion of hepatocellular carcinoma cells and reduces the sensitivity of hepatocellular carcinoma cells to 5-Fu and CDDP [27]. SSX2IP is predominantly positively correlated in our model. It has also been demonstrated in previous studies that upregulation of SSX2IP further promotes metastasis and drug resistance in hepatocellular carcinoma. This is consistent with the results analysed in this model.

The G2 and S phase-expressed-1 (GTSE1) is specifically expressed in the G2 and S phases of the cell cycle and it is located on chromosome 22q13.2-q13.3 [44]. A study found that the protein GTSE1 is predominantly located in the cytoplasm and is associated with the activity of cytoplasmic microtubule proteins and microtubules during mitosis [45]. Chromosome movement and spindle integrity are key steps in mitosis, and GTSE1 is a key regulator in this process [46]. In addition, GTSE1 is able to degrade P53 by binding to it and transporting it out of the nucleus [47, 48]. GTSE1 has been shown to be overexpressed in HCC and to act as a marker of poor prognosis. It not only reduces the sensitivity of HCC cells to 5-FU but also promotes malignant biological behavior of HCC by increasing the proliferation and metastatic capacity of HCC and upregulating it [28-30]. The patient treated with cisplatin for myeloma had his GTSE1 upregulated in the cells, leading to drug resistance. Patients treated with cisplatin for myeloma had their GTSE1 upregulated in cells, leading to drug resistance [49]. In addition, GTSE1 was able to inhibit apoptotic signaling of P53 in cells after cisplatin treatment in patients with gastric cancer [50]. It has been demonstrated that GTSE1 promotes metastasis, growth and confers multidrug resistance in breast cancer when upregulated [51-53]. The analysis revealed that GTSE1 is in this model and his upregulation promotes the progression of hepatocellular carcinoma. Interestingly, of all the studies that have been confirmed, we found that GTSE1 also promotes the progression of hepatocellular carcinoma.

SLC1A5 is a key component of the amino acid exchanger, which is also one of the genes with the highest aberrant expression and lymphocyte activation in cancer cells [54-59]. SLC1A5 is interrelated with DDR1 and regulates hepatocellular carcinoma progression through the mTORC1 signaling pathway. expression of SLC1A5 and DDR1 are positively correlated. in HCC DDR1 and SLC1A5 are upregulated [31, 60]. The STAT3-MYC axis has been reported to promote leukaemia stem cell survival, which is achieved through regulation of SLC1A5 and oxidative phosphorylation [61]. In addition, in the immune microenvironment, SLC1A5 is altered by the uptake of glutamine and thus the microenvironment. Therefore this would be a target for enhancing anti-tumour immune function [62]. In previous studies SLC1A5 has been shown to promote the development of hepatocellular

carcinoma mainly through the metabolism of glutamine. According to the model we have analysed, SLC1A5 also promotes hepatocellular carcinoma. The results of these two studies are equally consistent.

In summary, this study developed a prognostic model based on copper death and SARS-CoV-2 related genes. This model consisted of four genes. Three of these genes are directly influencing the development of hepatocellular carcinoma, while RNF145 is influencing cholesterol metabolism and thus indirectly influencing hepatocellular carcinoma. This prognostic model is therefore very reliable.

5. Conclusion

In this study, we have developed a prognostic model through copper death and SARS-CoV-2 related genes. This prognostic model has a high predictive power. Also, three of the four genes in the model have been directly involved in the development of liver cancer. And 1 gene is indirectly involved.

Declarations

Consent for publication

Not applicable

Availability of data and materials

Not applicable

Data Availability

The raw data supporting the conclusions of this article will be made available by the authors, without undue reservation.

ETHICS STATEMENT

Institutional ethics committee approval was not required for the current study for the TCGA and GEO are publicly available.

ORCID iD authorship contribution statement

Author Contributions Section: Congzhi Yan, Zhixuan Wu, and Donghao Lou, carried out the assays, studying the data to write the paper. Jingji Jin and Congcong Wu conceived our research and contributed experimental materials. Each researcher has read and polished the eventual paper.

Declaration of Competing Interest

The authors declare that they have no known competing financial interests or personal relationships that could have appeared to influence the work reported in this paper

Acknowledgments

We acknowledge TCGA for providing their platforms and contributors for uploading their meaningful datasets.

Funding

None

s, * $P < 0.05$. ** $P < 0.01$, *** $P < 0.001$, **** $P < 0.0001$

References

1. Ferlay J, Colombet M, Soerjomataram I, Mathers C, Parkin DM, Pineros M, Znaor A, Bray F: **Estimating the global cancer incidence and mortality in 2018: GLOBOCAN sources and methods.** *Int J Cancer* 2019, **144**(8):1941–1953.
2. Xu Y, Guo Q, Wei L: **The Emerging Influences of Alpha-Fetoprotein in the Tumorigenesis and Progression of Hepatocellular Carcinoma.** *Cancers (Basel)* 2021, **13**(20).
3. Debes JD, Romagnoli PA, Prieto J, Arrese M, Mattos AZ, Boonstra A, On Behalf Of The Escalon C: **Serum Biomarkers for the Prediction of Hepatocellular Carcinoma.** *Cancers (Basel)* 2021, **13**(7).
4. Hu X, Chen R, Wei Q, Xu X: **The Landscape Of Alpha Fetoprotein In Hepatocellular Carcinoma: Where Are We?** *Int J Biol Sci* 2022, **18**(2):536–551.
5. Pelizzaro F, Cardin R, Penzo B, Pinto E, Vitale A, Cillo U, Russo FP, Farinati F: **Liquid Biopsy in Hepatocellular Carcinoma: Where Are We Now?** *Cancers (Basel)* 2021, **13**(9).
6. Sachar Y, Brahmania M, Dhanasekaran R, Congly SE: **Screening for Hepatocellular Carcinoma in Patients with Hepatitis B.** *Viruses* 2021, **13**(7).
7. European Association for the Study of the Liver. Electronic address eee, European Association for the Study of the L: **EASL Clinical Practice Guidelines: Management of hepatocellular carcinoma.** *J Hepatol* 2018, **69**(1):182–236.
8. Llovet JM, Castet F, Heikenwalder M, Maini MK, Mazzaferro V, Pinato DJ, Pikarsky E, Zhu AX, Finn RS: **Immunotherapies for hepatocellular carcinoma.** *Nat Rev Clin Oncol* 2022, **19**(3):151–172.
9. Sangro B, Sarobe P, Hervas-Stubbs S, Melero I: **Advances in immunotherapy for hepatocellular carcinoma.** *Nat Rev Gastroenterol Hepatol* 2021, **18**(8):525–543.
10. Llovet JM, De Baere T, Kulik L, Haber PK, Greten TF, Meyer T, Lencioni R: **Locoregional therapies in the era of molecular and immune treatments for hepatocellular carcinoma.** *Nat Rev Gastroenterol Hepatol* 2021, **18**(5):293–313.
11. Mohr R, Jost-Brinkmann F, Ozdirik B, Lambrecht J, Hammerich L, Loosen SH, Luedde T, Demir M, Tacke F, Roderburg C: **Lessons From Immune Checkpoint Inhibitor Trials in Hepatocellular Carcinoma.** *Front Immunol* 2021, **12**:652172.
12. Singh A, Beechinor RJ, Huynh JC, Li D, Dayyani F, Valerin JB, Hendifar A, Gong J, Cho M: **Immunotherapy Updates in Advanced Hepatocellular Carcinoma.** *Cancers (Basel)* 2021, **13**(9).
13. Siegel RL, Miller KD, Fuchs HE, Jemal A: **Cancer statistics, 2022.** *CA Cancer J Clin* 2022, **72**(1):7–33.
14. Kim BE, Nevitt T, Thiele DJ: **Mechanisms for copper acquisition, distribution and regulation.** *Nat Chem Biol* 2008, **4**(3):176–185.
15. Ge EJ, Bush AI, Casini A, Cobine PA, Cross JR, DeNicola GM, Dou QP, Franz KJ, Gohil VM, Gupta S *et al.*: **Connecting copper and cancer: from transition metal signalling to metalloplasia.** *Nat Rev Cancer* 2022, **22**(2):102–113.
16. Lutsenko S: **Human copper homeostasis: a network of interconnected pathways.** *Curr Opin Chem Biol* 2010, **14**(2):211–217.
17. Rae TD, Schmidt PJ, Pufahl RA, Culotta VC, O'Halloran TV: **Undetectable intracellular free copper: the requirement of a copper chaperone for superoxide dismutase.** *Science* 1999, **284**(5415):805–808.
18. Tsvetkov P, Coy S, Petrova B, Dreishpoon M, Verma A, Abdusamad M, Rossen J, Joesch-Cohen L, Humeidi R, Spangler RD *et al.*: **Copper induces cell death by targeting lipoylated TCA cycle proteins.** *Science* 2022, **375**(6586):1254–1261.
19. Holmes EC, Goldstein SA, Rasmussen AL, Robertson DL, Crits-Christoph A, Wertheim JO, Anthony SJ, Barclay WS, Boni MF, Doherty PC *et al.*: **The origins of SARS-CoV-2: A critical review.** *Cell* 2021, **184**(19):4848–4856.
20. Jackson CB, Farzan M, Chen B, Choe H: **Mechanisms of SARS-CoV-2 entry into cells.** *Nat Rev Mol Cell Biol* 2022, **23**(1):3–20.
21. Creech CB, Walker SC, Samuels RJ: **SARS-CoV-2 Vaccines.** *JAMA* 2021, **325**(13):1318–1320.
22. Gupta RK: **Will SARS-CoV-2 variants of concern affect the promise of vaccines?** *Nat Rev Immunol* 2021, **21**(6):340–341.
23. Golob JL, Lugogo N, Luring AS, Lok AS: **SARS-CoV-2 vaccines: a triumph of science and collaboration.** *JCI Insight* 2021, **6**(9).

24. Chakraborty S, Mallajosyula V, Tato CM, Tan GS, Wang TT: **SARS-CoV-2 vaccines in advanced clinical trials: Where do we stand?** *Adv Drug Deliv Rev* 2021, **172**:314–338.
25. Cohen JI, Burbelo PD: **Reinfection With SARS-CoV-2: Implications for Vaccines.** *Clin Infect Dis* 2021, **73**(11):e4223–e4228.
26. Rooney MS, Shukla SA, Wu CJ, Getz G, Hacohen N: **Molecular and genetic properties of tumors associated with local immune cytolytic activity.** *Cell* 2015, **160**(1–2):48–61.
27. Li P, Lin Y, Zhang Y, Zhu Z, Huo K: **SSX2IP promotes metastasis and chemotherapeutic resistance of hepatocellular carcinoma.** *J Transl Med* 2013, **11**:52.
28. Li SS, Chen DM, Chen LB, Wei H, Wang JL, Xiao J, Huang YH, Lian YF: **GTSE1 promotes SNAIL1 degradation by facilitating its nuclear export in hepatocellular carcinoma cells.** *Mol Med Rep* 2021, **23**(6).
29. Guo L, Zhang S, Zhang B, Chen W, Li X, Zhang W, Zhou C, Zhang J, Ren N, Ye Q: **Silencing GTSE-1 expression inhibits proliferation and invasion of hepatocellular carcinoma cells.** *Cell Biol Toxicol* 2016, **32**(4):263–274.
30. Wu X, Wang H, Lian Y, Chen L, Gu L, Wang J, Huang Y, Deng M, Gao Z, Huang Y: **GTSE1 promotes cell migration and invasion by regulating EMT in hepatocellular carcinoma and is associated with poor prognosis.** *Sci Rep* 2017, **7**(1):5129.
31. Pan Y, Han M, Zhang X, He Y, Yuan C, Xiong Y, Li X, Zeng C, Lu K, Zhu H *et al*: **Discoidin domain receptor 1 promotes hepatocellular carcinoma progression through modulation of SLC1A5 and the mTORC1 signaling pathway.** *Cell Oncol (Dordr)* 2022, **45**(1):163–178.
32. Du D, Liu C, Qin M, Zhang X, Xi T, Yuan S, Hao H, Xiong J: **Metabolic dysregulation and emerging therapeutical targets for hepatocellular carcinoma.** *Acta Pharm Sin B* 2022, **12**(2):558–580.
33. Yang H, Li G, Qiu G: **Bioinformatics Analysis Using ATAC-seq and RNA-seq for the Identification of 15 Gene Signatures Associated With the Prediction of Prognosis in Hepatocellular Carcinoma.** *Front Oncol* 2021, **11**:726551.
34. Cook EC, Nelson JK, Sorrentino V, Koenis D, Moeton M, Scheij S, Ottenhoff R, Bleijlevens B, Loregger A, Zelcer N: **Identification of the ER-resident E3 ubiquitin ligase RNF145 as a novel LXR-regulated gene.** *PLoS One* 2017, **12**(2):e0172721.
35. Zhang L, Rajbhandari P, Priest C, Sandhu J, Wu X, Temel R, Castrillo A, de Aguiar Vallim TQ, Sallam T, Tontonoz P: **Inhibition of cholesterol biosynthesis through RNF145-dependent ubiquitination of SCAP.** *Elife* 2017, **6**.
36. Zhang A, Guan Z, Ockerman K, Dong P, Guo J, Wang Z, Yan D: **Regulation of glial size by eicosapentaenoic acid through a novel Golgi apparatus mechanism.** *PLoS Biol* 2020, **18**(12):e3001051.
37. Jiang LY, Jiang W, Tian N, Xiong YN, Liu J, Wei J, Wu KY, Luo J, Shi XJ, Song BL: **Ring finger protein 145 (RNF145) is a ubiquitin ligase for sterol-induced degradation of HMG-CoA reductase.** *J Biol Chem* 2018, **293**(11):4047–4055.
38. Ming J, Wei X, Han M, Adi D, Abuzhalihan J, Wang YT, Yang YN, Li XM, Xie X, Fu ZY *et al*: **Genetic variation of RNF145 gene and blood lipid levels in Xinjiang population, China.** *Sci Rep* 2021, **11**(1):5969.
39. Zhang X, Coker OO, Chu ES, Fu K, Lau HCH, Wang YX, Chan AWH, Wei H, Yang X, Sung JJY *et al*: **Dietary cholesterol drives fatty liver-associated liver cancer by modulating gut microbiota and metabolites.** *Gut* 2021, **70**(4):761–774.
40. Liang JQ, Teoh N, Xu L, Pok S, Li X, Chu ESH, Chiu J, Dong L, Arfianti E, Haigh WG *et al*: **Dietary cholesterol promotes steatohepatitis related hepatocellular carcinoma through dysregulated metabolism and calcium signaling.** *Nat Commun* 2018, **9**(1):4490.
41. Chang SL, Lee SW, Yang SF, Chien CC, Chan TC, Chen TJ, Yang CC, Li CF, Wei YC: **Expression and prognostic utility of SSX2IP in patients with nasopharyngeal carcinoma.** *APMIS* 2020, **128**(4):287–297.
42. Guinn B, Greiner J, Schmitt M, Mills KI: **Elevated expression of the leukemia-associated antigen SSX2IP predicts survival in acute myeloid leukemia patients who lack detectable cytogenetic rearrangements.** *Blood* 2009, **113**(5):1203–1204.
43. Li P, Chen X, Su L, Li C, Zhi Q, Yu B, Sheng H, Wang J, Feng R, Cai Q *et al*: **Epigenetic silencing of miR-338-3p contributes to tumorigenicity in gastric cancer by targeting SSX2IP.** *PLoS One* 2013, **8**(6):e66782.
44. Monte M, Collavin L, Lazarevic D, Utrera R, Dragani TA, Schneider C: **Cloning, chromosome mapping and functional characterization of a human homologue of murine gtse-1 (B99) gene.** *Gene* 2000, **254**(1–2):229–236.

45. Monte M, Benetti R, Buscemi G, Sandy P, Del Sal G, Schneider C: **The cell cycle-regulated protein human GTSE-1 controls DNA damage-induced apoptosis by affecting p53 function.** *J Biol Chem* 2003, **278**(32):30356–30364.
46. Tipton AR, Wren JD, Daum JR, Siefert JC, Gorbsky GJ: **GTSE1 regulates spindle microtubule dynamics to control Aurora B kinase and Kif4A chromokinesin on chromosome arms.** *J Cell Biol* 2017, **216**(10):3117–3132.
47. Collavin L, Monte M, Verardo R, Pfleger C, Schneider C: **Cell-cycle regulation of the p53-inducible gene B99.** *FEBS Lett* 2000, **481**(1):57–62.
48. Monte M, Benetti R, Collavin L, Marchionni L, Del Sal G, Schneider C: **hGTSE-1 expression stimulates cytoplasmic localization of p53.** *J Biol Chem* 2004, **279**(12):11744–11752.
49. Xu T, Ma M, Chi Z, Si L, Sheng X, Cui C, Dai J, Yu S, Yan J, Yu H *et al*: **High G2 and S-phase expressed 1 expression promotes acral melanoma progression and correlates with poor clinical prognosis.** *Cancer Sci* 2018, **109**(6):1787–1798.
50. Subhash VV, Tan SH, Tan WL, Yeo MS, Xie C, Wong FY, Kiat ZY, Lim R, Yong WP: **GTSE1 expression represses apoptotic signaling and confers cisplatin resistance in gastric cancer cells.** *BMC Cancer* 2015, **15**:550.
51. Stelitano D, Peche LY, Dalla E, Monte M, Piazza S, Schneider C: **GTSE1: a novel TEAD4-E2F1 target gene involved in cell protrusions formation in triple-negative breast cancer cell models.** *Oncotarget* 2017, **8**(40):67422–67438.
52. Bartucci M, Dattilo R, Moriconi C, Pagliuca A, Mottolese M, Federici G, Benedetto AD, Todaro M, Stassi G, Sperati F *et al*: **TAZ is required for metastatic activity and chemoresistance of breast cancer stem cells.** *Oncogene* 2015, **34**(6):681–690.
53. Lin F, Xie YJ, Zhang XK, Huang TJ, Xu HF, Mei Y, Liang H, Hu H, Lin ST, Luo FF *et al*: **GTSE1 is involved in breast cancer progression in p53 mutation-dependent manner.** *J Exp Clin Cancer Res* 2019, **38**(1):152.
54. O'Sullivan D, Sanin DE, Pearce EJ, Pearce EL: **Metabolic interventions in the immune response to cancer.** *Nat Rev Immunol* 2019, **19**(5):324–335.
55. Grzes KM, Swamy M, Hukelmann JL, Emslie E, Sinclair LV, Cantrell DA: **Control of amino acid transport coordinates metabolic reprogramming in T-cell malignancy.** *Leukemia* 2017, **31**(12):2771–2779.
56. Jensen H, Potempa M, Gotthardt D, Lanier LL: **Cutting Edge: IL-2-Induced Expression of the Amino Acid Transporters SLC1A5 and CD98 Is a Prerequisite for NKG2D-Mediated Activation of Human NK Cells.** *J Immunol* 2017, **199**(6):1967–1972.
57. McCracken AN, Edinger AL: **Nutrient transporters: the Achilles' heel of anabolism.** *Trends Endocrinol Metab* 2013, **24**(4):200–208.
58. Nakaya M, Xiao Y, Zhou X, Chang JH, Chang M, Cheng X, Blonska M, Lin X, Sun SC: **Inflammatory T cell responses rely on amino acid transporter ASCT2 facilitation of glutamine uptake and mTORC1 kinase activation.** *Immunity* 2014, **40**(5):692–705.
59. Nicklin P, Bergman P, Zhang B, Triantafellow E, Wang H, Nyfeler B, Yang H, Hild M, Kung C, Wilson C *et al*: **Bidirectional transport of amino acids regulates mTOR and autophagy.** *Cell* 2009, **136**(3):521–534.
60. Zhu R, Li X, Cai Z, Liang S, Yuan Y, Xu Y, Lai D, Zhao H, Yang W, Bian J *et al*: **Risk Scores Based on Six Survival-Related RNAs in a Competing Endogenous Network Composed of Differentially Expressed RNAs Between Clear Cell Renal Cell Carcinoma Patients Carrying Wild-Type or Mutant Von Hippel-Lindau Serve Well to Predict Malignancy and Prognosis.** *Front Oncol* 2021, **11**:726671.
61. Amaya ML, Inguva A, Pei S, Jones C, Krug A, Ye H, Minhajuddin M, Winters A, Furtek SL, Gamboni F *et al*: **The STAT3-MYC axis promotes survival of leukemia stem cells by regulating SLC1A5 and oxidative phosphorylation.** *Blood* 2022, **139**(4):584–596.
62. Nachev M, Ali AK, Almutairi SM, Lee SH: **Targeting SLC1A5 and SLC3A2/SLC7A5 as a Potential Strategy to Strengthen Anti-Tumor Immunity in the Tumor Microenvironment.** *Front Immunol* 2021, **12**:624324.

Tables

Table 1

	TCGA	GSE54236
Number	377	81
Survival time (average)	809.75	292.74
Age (average)	59.45	\
Grade1	55	\
Grade 2	108	\
Grade 3	124	\
Grade 4	13	\
Unknow	5	\
Stage I	175	\
Stage II	87	\
Stage III	86	\
Stage IV	5	\
Unknow	24	\
T1	185	\
T2	95	\
T3	81	\
T4	13	\
Unknow	3	\
M0	272	\
M1	4	\
Unknow	101	\
N0	257	\
N1	4	\
Unknow	116	\

Figures

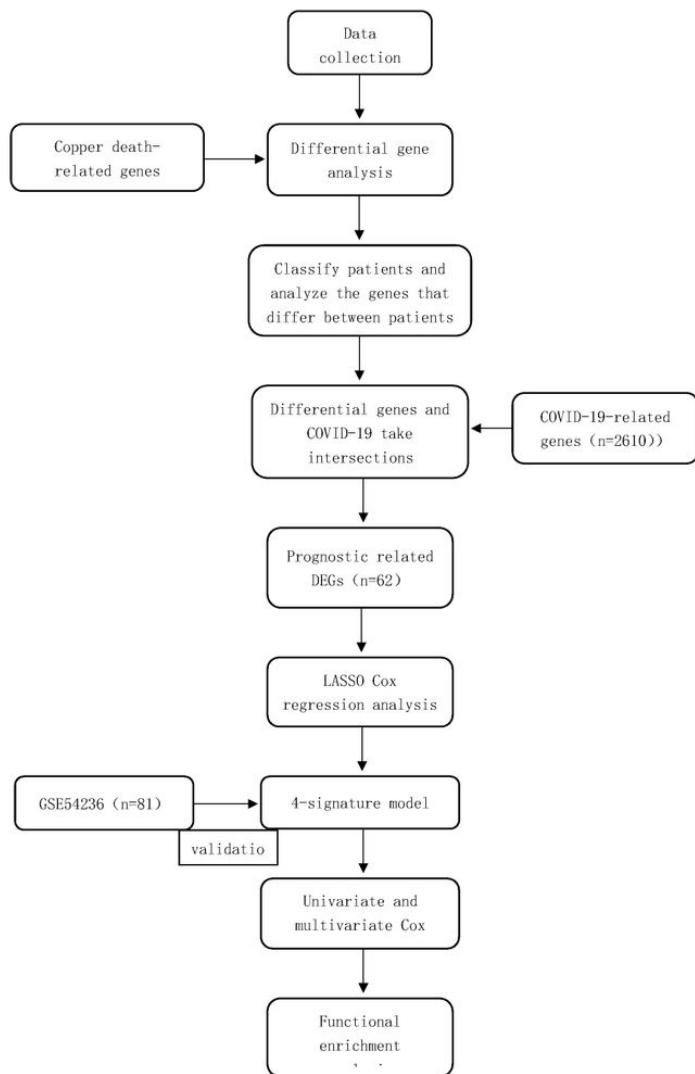


Figure 1

work of flow in this study

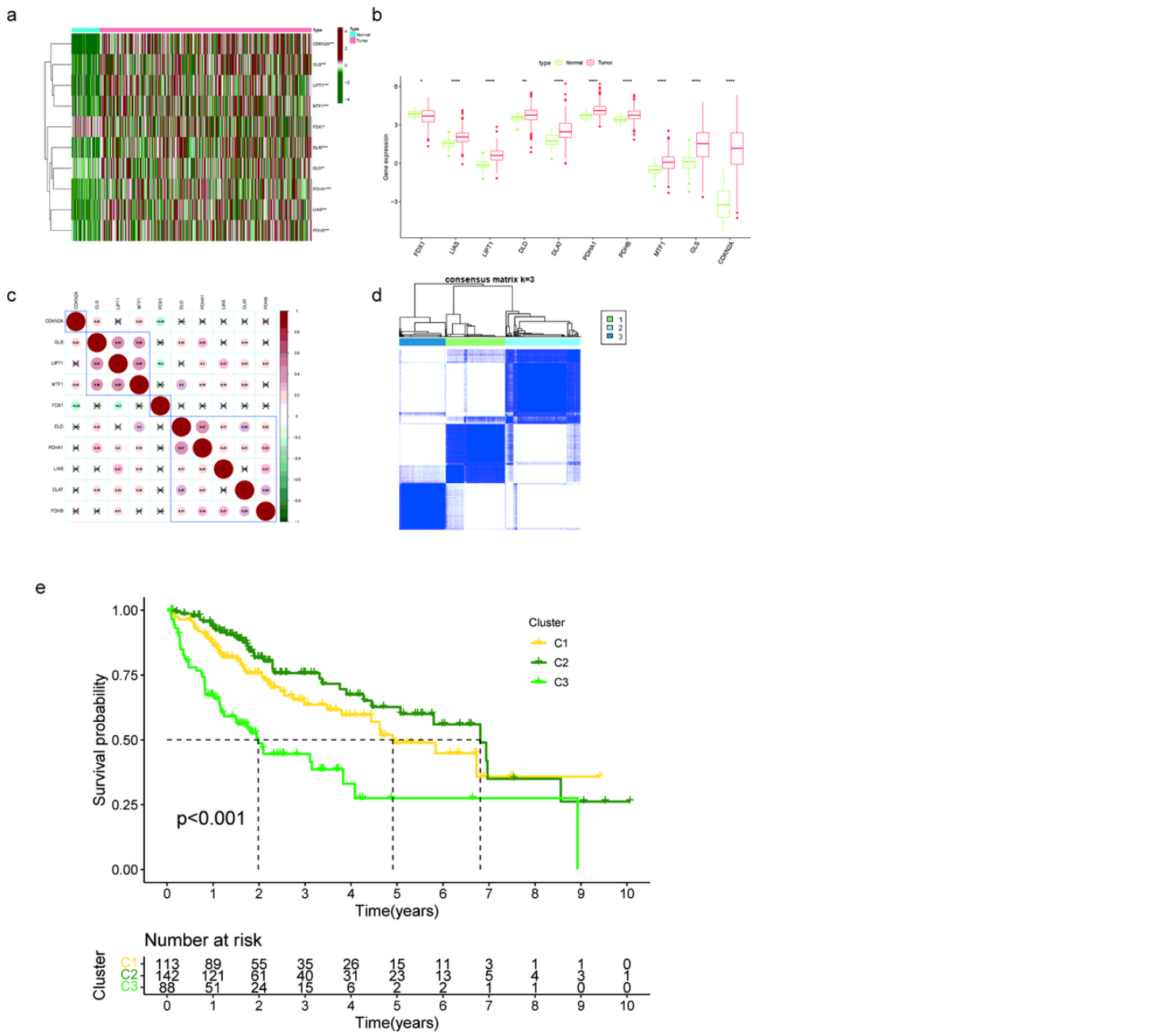


Figure 2

Identification of differentially expressed genes **a** Expression of 10 copper death-associated genes in hepatocellular carcinoma **b** Box line plot of differential expression of 10 copper death-related genes in normal tissue and hepatocellular carcinoma **c** Correlation between 10 copper death-associated genes **d** Breakdown of the three categories of patients **e** Kaplan-Meier curve between three types of patients.

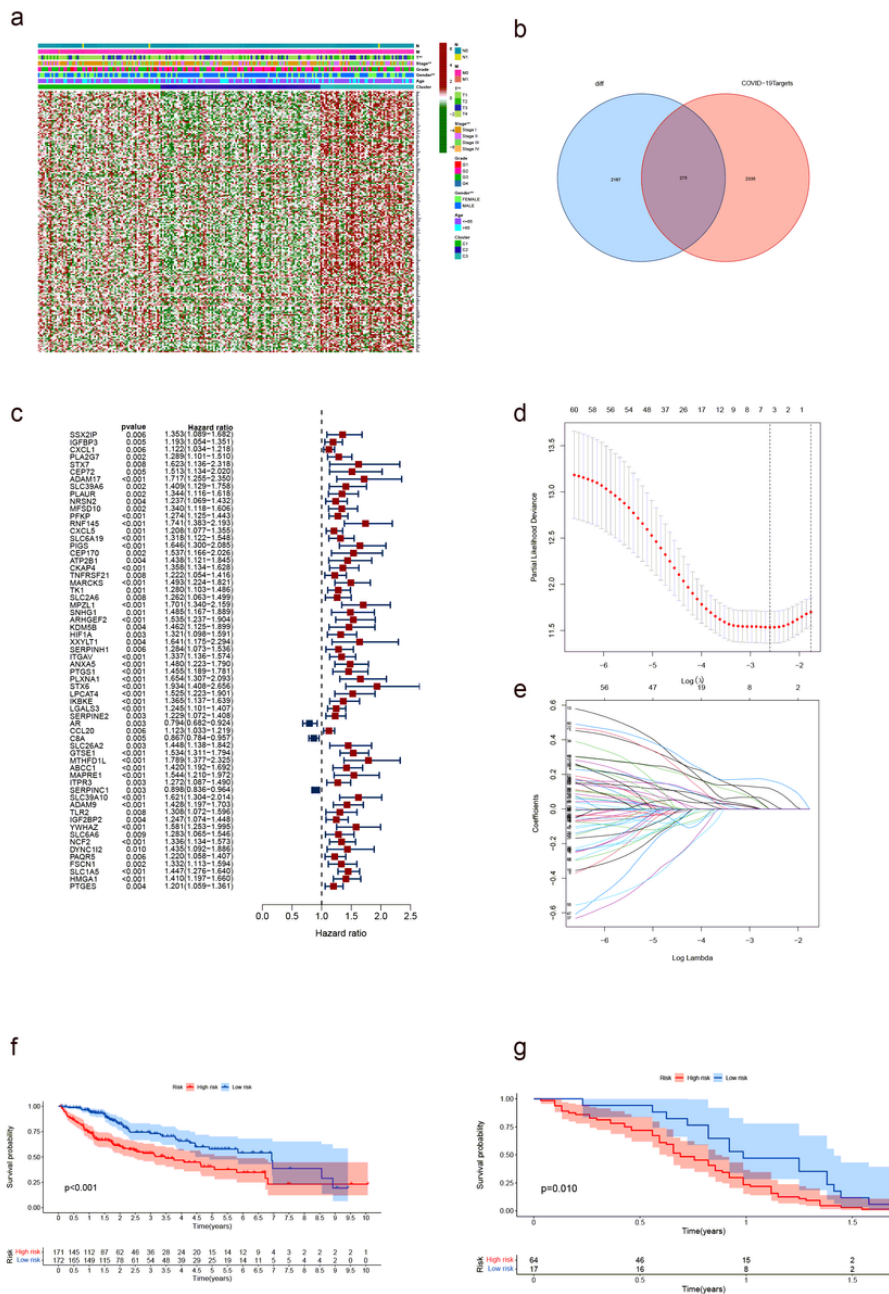


Figure 3

Identification and validation of prognostic models (a) Heat map of differential gene expression profiles and clinical features, (b) Intersecting genes for differential and COVID-19-related genes, (c) Genes associated with prognosis, (d) lasso regression analysis and (e) lasso regression models, (f) Kaplan-Meier curve for the training group (TCGA) and (g) the testing group (GEO).

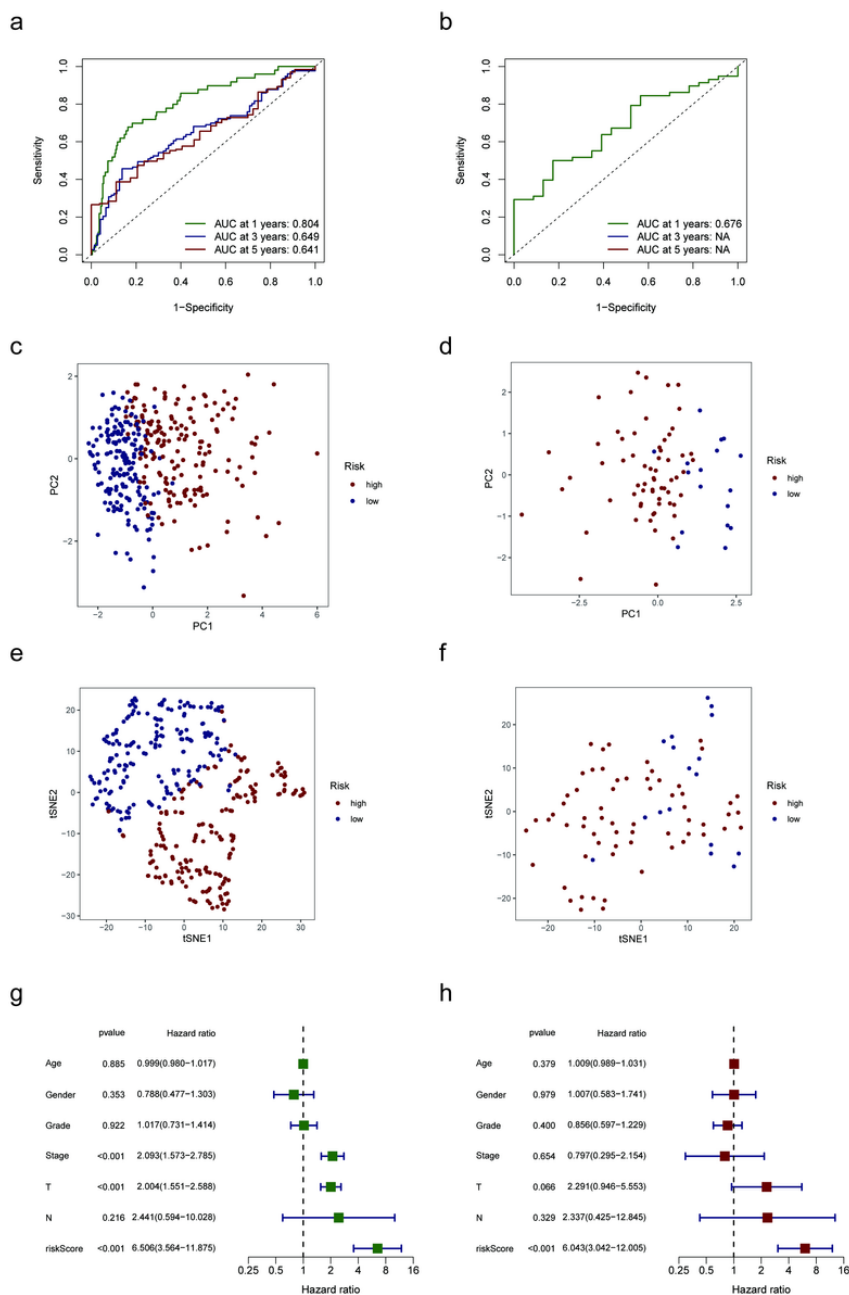


Figure 4

Area under the curve for the training(a) and validation groups(b), PCA for the training(c) and validation groups(d), t-SNE for the training(e) and validation groups(f), A forest plot of univariate Cox regression analysis in the cohorts(g). A forest plot of multivariate Cox regression analysis in the cohorts(h).

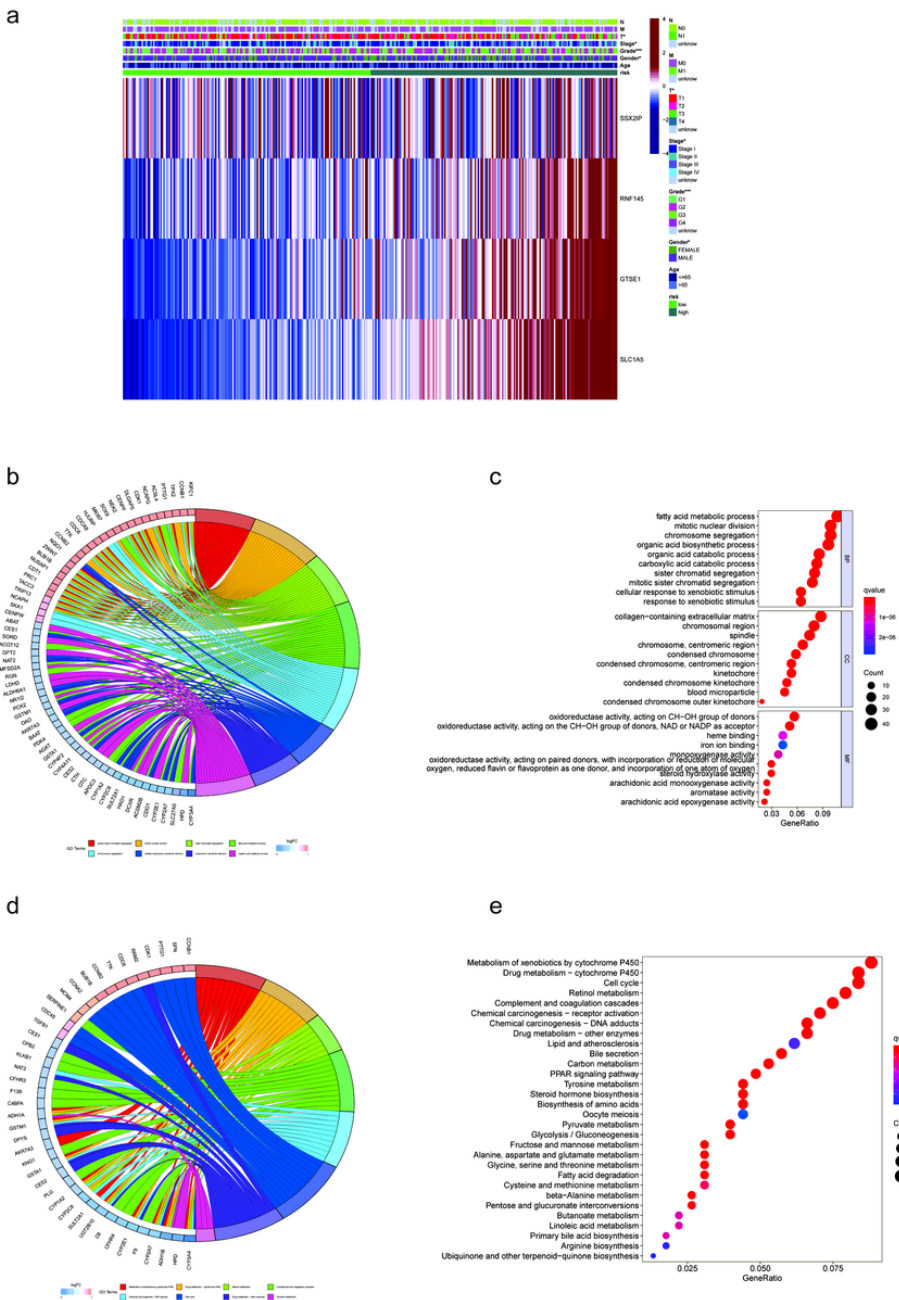


Figure 5

(a) Heat map of 4 prognostic model genes and clinical features, (b) GO clustering map of differential genes, (c) GO bubble plots for the top 30 genes, (d) KEGG clustering map of differential genes, (f) KEGG bubble plots for the top 30 genes.

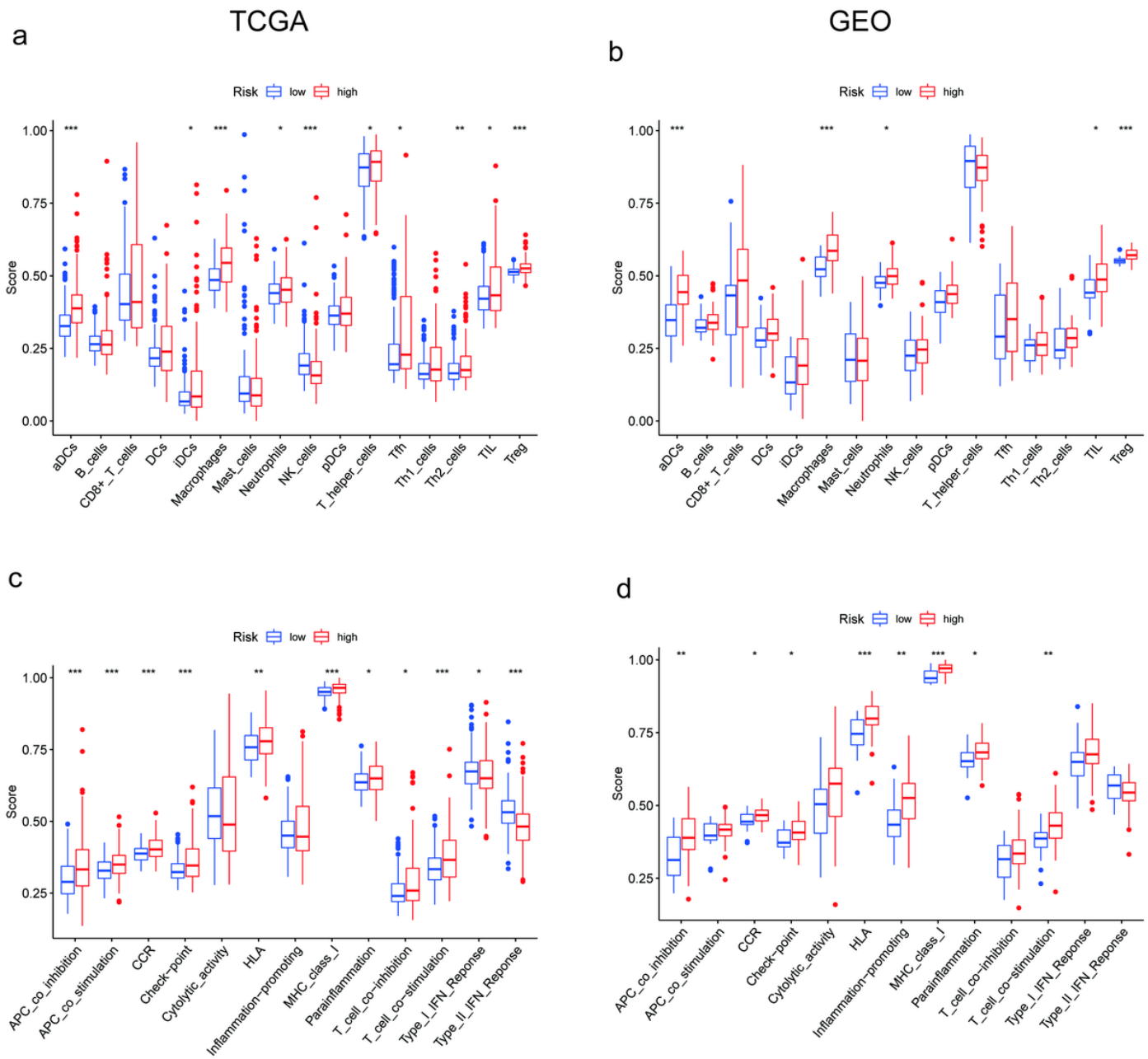


Figure 6

Infiltration of 16 types of immune cells in TCGA(a) and GEO(b), Differential expression of 13 immune-related pathways in TCGA(c) and GEO(d).

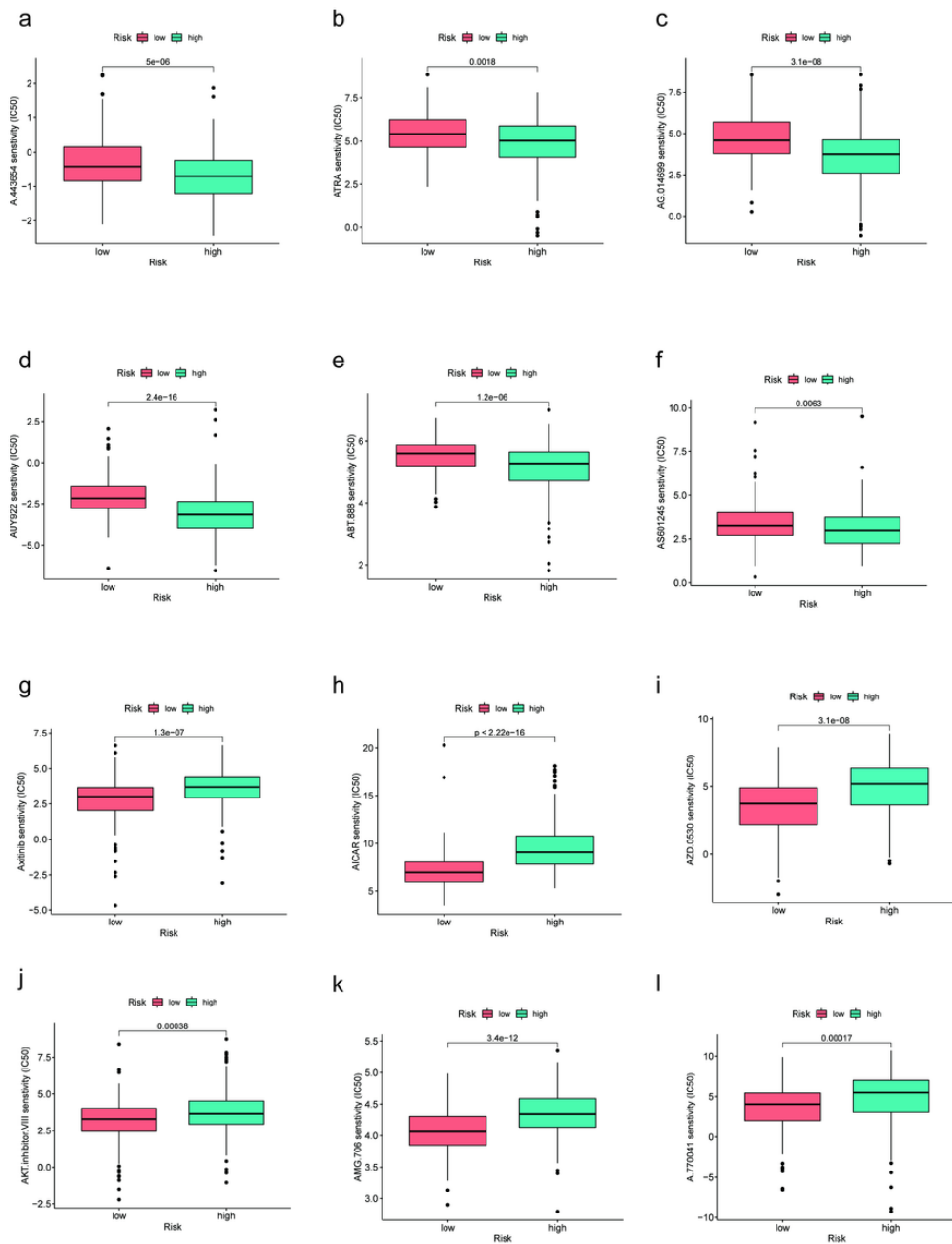


Figure 7

Differences in sensitivity between the 12 drugs in the high and low risk groups.

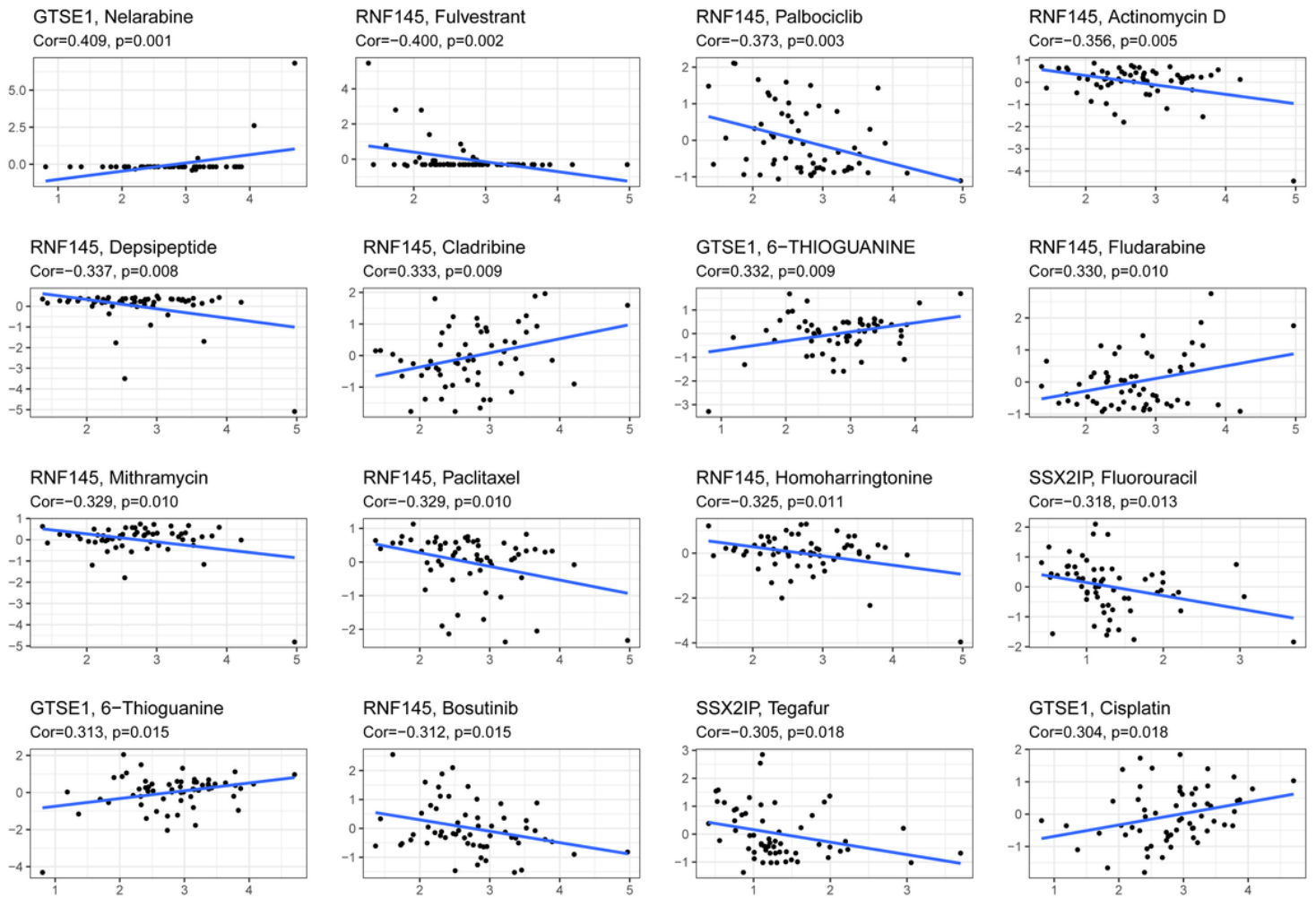


Figure 8

Correlation between genes and drugs